Search for Novel Aminoglycosides by Combining Fragment-Based Virtual Screening and 3D-QSAR Scoring

Piotr Setny*,†,‡ and Joanna Trylska†

Interdisciplinary Centre for Mathematical and Computational Modelling and Faculty of Physics, University of Warsaw, Warsaw 02-089, Poland

Received October 2, 2008

Aminoglycosides are antibiotics targeting the 16S RNA A site of the bacterial ribosome. There have been many efforts directed toward design of their synthetic derivatives, however with only few successes. As RNA binders, aminoglycosides are also a difficult target for computational drug design, since most of the existing methods were developed for protein ligands. Here, we present an approach that allows for evading the problems related to still poorly developed RNA docking and scoring algorithms. It is aimed at identification of new molecular scaffolds potentially binding to the A site. The considered molecules are based on the neamine core, which is common for all aminoglycosides and provides specificity toward the binding site, linked with diverse molecular fragments via its O5 or O6 oxygen atom. Suitable fragments are selected with the use of 3D searches of molecular fragments library against two distinct pharmacophores designed on the basis of available structural data for aminoglycoside-RNA complexes. The compounds resulting from fragments assembly with neamine are then scored with a 3D-QSAR model developed using the biological data for known aminoglycoside derivatives. Twenty-one new potential ligands are obtained, four of which have predicted activities comparable to less potent aminoglycoside antibiotics.

INTRODUCTION

The increasing bacterial resistance to existing antibiotics highlights the need for constant development of new therapeutic agents.[1] One of the main targets for antibacterial drugs is the prokaryotic ribosome.[2,3] The ribosome is a large ribonucleoprotein complex responsible in the cell for translation i.e., the synthesis of polypeptide chains on the basis of information carried by mRNA.

Among clinically relevant classes of antibiotics targeting different stages of translation, aminoglycosides are one of the most thoroughly investigated.[4] They are effective, broad spectrum bactericidal antibiotics, which despite growing bacterial resistance[5] and considerable toxicity,[4] are used in hospitals against particularly severe infections. Still, it is highly desirable to obtain novel synthetic compounds that would be more potent and selective, while being better tolerated by the host organism.

From the chemical point of view, aminoglycosides are oligosaccharides, containing a variable number of sugar rings with attached amino groups—typically 3 to 6 rings per compound. They all share a common 2-deoxystreptamine ring (2-DOS; ring II) and a more variable ring I, linked to it at position 4. Together, both rings constitute a neamine core (Figure 1). The nature of the second chemical linkage with ring II gives rise to two distinct classes of aminoglycosides: 4,5 disubstituted 2-DOS derivatives (including ribostamycin, paromomycin, neomycin, and lividomycin) and 4,6 disubstituted 2-DOS derivatives (including tobramycin, kanamycin, Geneticin, and gentamicin) (Figure 3, D).

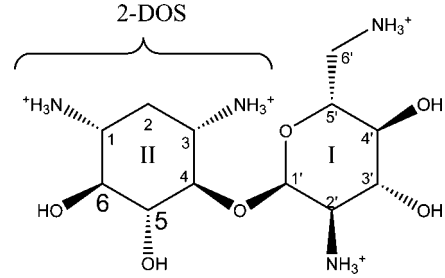

Figure 1. The neamine moiety, showing 2-deoxystreptamine ring (2-DOS—ring II) with O5 and O6 oxygens, used as anchor points for the considered substituents.

A number of structural[6−11] and thermodynamic[12−17] data exist, providing insight into aminoglycoside binding mode and action. Aminoglycosides bind to the 16S rRNA, at the double helix of aminoacyl-tRNA decoding site (A site).[18] In each case, the neamine core adopts a virtually identical position within the binding site.[19] The ring I is inserted into the helix, where it stacks over guanine G1491, and forms a pseudobase pair with adenine A1408. Amino groups of ring II form hydrogen bonds with the universally conserved U1406·U1495 pair as well as with guanine G1494 and a phosphate group of adenine A1493. Additional contacts, formed by the remaining rings, are more diverse, reflecting the variability of neamine substituents. Some of the contacts are also mediated by individual water molecules, whose presence is important for the plasticity of RNA—aminoglycoside recognition due to increasing the diversity of ligands that can be successfully accommodated.

All the amino groups carried by aminoglycosides are positively charged at physiological pH.[14] The large part of the total charge (+4*e*) remains on the neamine core,

* Corresponding author e-mail: piosto@icm.edu.pl.
† Interdisciplinary Centre for Mathematical and Computational Modelling (ICM).
‡ Faculty of Physics.

10.1021/ci800361a CCC: $40.75
Published on Web 01/27/2009

augmenting its role as an anchor fragment for binding to the negatively charged RNA. Although the total charge positively correlates with binding affinity,[17] it appears to be somewhat less important for biological activity.[14] Furthermore, it is deemed responsible for aminoglycoside toxicity.[3]

The molecular mechanism of aminoglycoside bactericidal action is related to their intrahelical binding to the A-site. Upon binding, the neamine core promotes stabilization of two adenine bases (A1492 and A1493) in an extrahelical conformation which increases their favorable interaction with tRNA. As an effect, ribosome's ability to discriminate between cognate and noncognate tRNA is decreased, which in turn reduces the fidelity of the translation process, and leads to the death of the bacterial cell.

Because a great deal is known about aminoglycoside's structure and function in the A-site, one would expect considerable progress in the design of potent aminoglycoside derivatives. However, on the contrary, successes in this field are rather sparse.[20,21] One of the very few notable examples is amikacin—a potent, semisynthetic antibiotic, reserved for hospital treatment of particularly severe infections.

In most strategies applied to obtain novel A-site binders, the importance of the neamine core is recognized. Some of the systematic approaches aim at its modifications that preserve the original interaction pattern.[22−25] Others leave the core mostly untouched and focus on its substituents.[26−31]

In the past few years, the availability of structural data of aminoglycoside-RNA complexes has also allowed for structure-based, computational approaches. Mobashery and co-workers[32] considered a receptor site, consisting of the aminoglycoside binding pocket with bound paromomycin rings I and II, and performed a random search of 273,000 compounds from the Cambridge Structural Database and the National Cancer Institute Database. The promising binders were then assembled with the neamine analogue and experimentally tested for their A-site affinity and biological activity. Foloppe and co-workers[33] performed a computational screening of more than 1 million compounds against a crystal structure of the A-site. From the resulting binders, representing completely new and diverse scaffolds, one molecule had close contacts with key nucleotides of the binding pocket, confirmed by NMR.

Given the amount of available data, and the overall interest in the discovery of new A-site ligands, computational attempts in this area are noticeably less frequent than one would expect. But it should be noted that RNA docking and scoring still pose a significant challenge. To date, most computational methods have been developed and parametrized for protein−ligand systems, and they cannot be easily transferred to the RNA world.[34] Among important issues are the flexibility of RNA−ligand complexes and the presence of many localized water molecules, often bridging the critically important interactions. Also, the chemical nature of RNA, promoting highly charged ligands and, unlike proteins, offering little or no hydrophobic contacts, requires completely new scoring functions. Although the first attempts to address those issues are visible,[34−36] we decided to use a different approach, allowing, at least in part, for the minimization of their impact on the results.

The aim of our study was to develop a computational approach to screen a possibly diverse set of small molecular structures, in order to obtain scaffolds capable of fitting into the A-site upon their linking with the neamine core. The resulting candidates for novel compounds should hopefully benefit from specificity provided by the neamine as well as affinity resulting from reproducing the key interactions, otherwise maintained by aminoglycoside rings III and IV. Our strategy was to exploit both O5 and O6 neamine oxygen atoms as the attachment points for new possible substituents. We performed a pharmacophoric search with subsequent QSAR-based assessment of activities of the obtained compounds. Such a method allows combining receptor-based and ligand-based approaches, thus utilizing most of the currently available structural data, while at the same time avoiding problems associated with RNA docking and scoring.

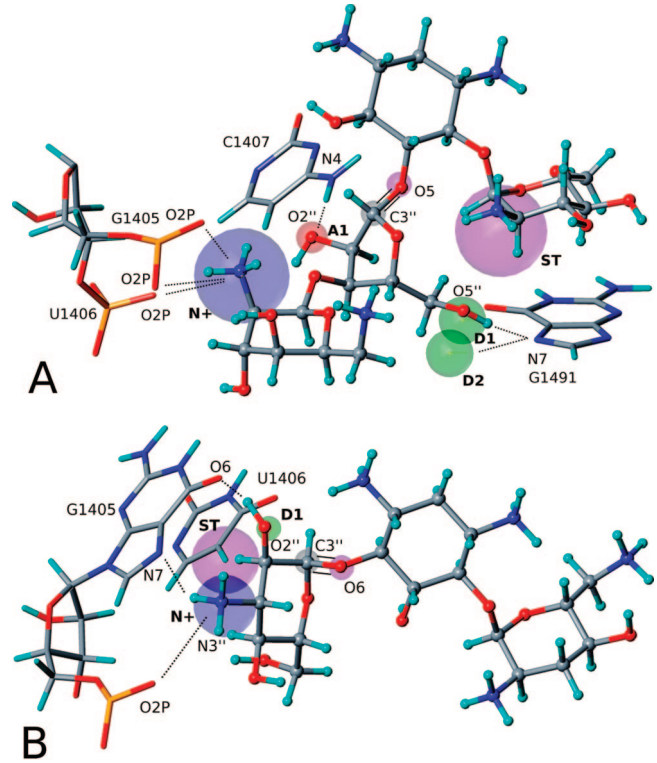

Figure 2. Pharmacophores for a) 4,5 disubstituted 2-DOS derivatives (paromomomycin is shown as a template) and b) 4,6 disubstituted 2-DOS derivatives (tobramycin is shown as a template). Red spheres: hydrogen bond acceptors, green spheres: hydrogen bond donors, blue spheres: positive nitrogen atom, violet spheres: steric features corresponding to receptor atoms. Small gray and violet spheres denote positions of atoms necessary to form a bond with oxygens O5 or O6.

METHODS

Screening Procedure. *Pharmacophore Construction.* A separate pharmacophore was designed for each of the two considered attachment points. Pharmacophoric features were derived based on the analysis of aligned crystal structures of aminoglycosides bound to 16S RNA and the selection of the most recurrent interaction motifs. The crystal structure of paromomycin bound to 16S RNA (PDB entry 1J7T) was used as a template for the alignment and for subsequent pharmacophore construction.

In case of 4,5 disubstituted 2-DOS derivatives, the following pharmacophoric features were considered (Figure 2, a): hydrogen bond acceptor, interacting with N4 nitrogen of C1407 (also allowed to be a hydroxyl group oxygen), a hydrogen bond donor, interacting with N7 nitrogen of G1491,

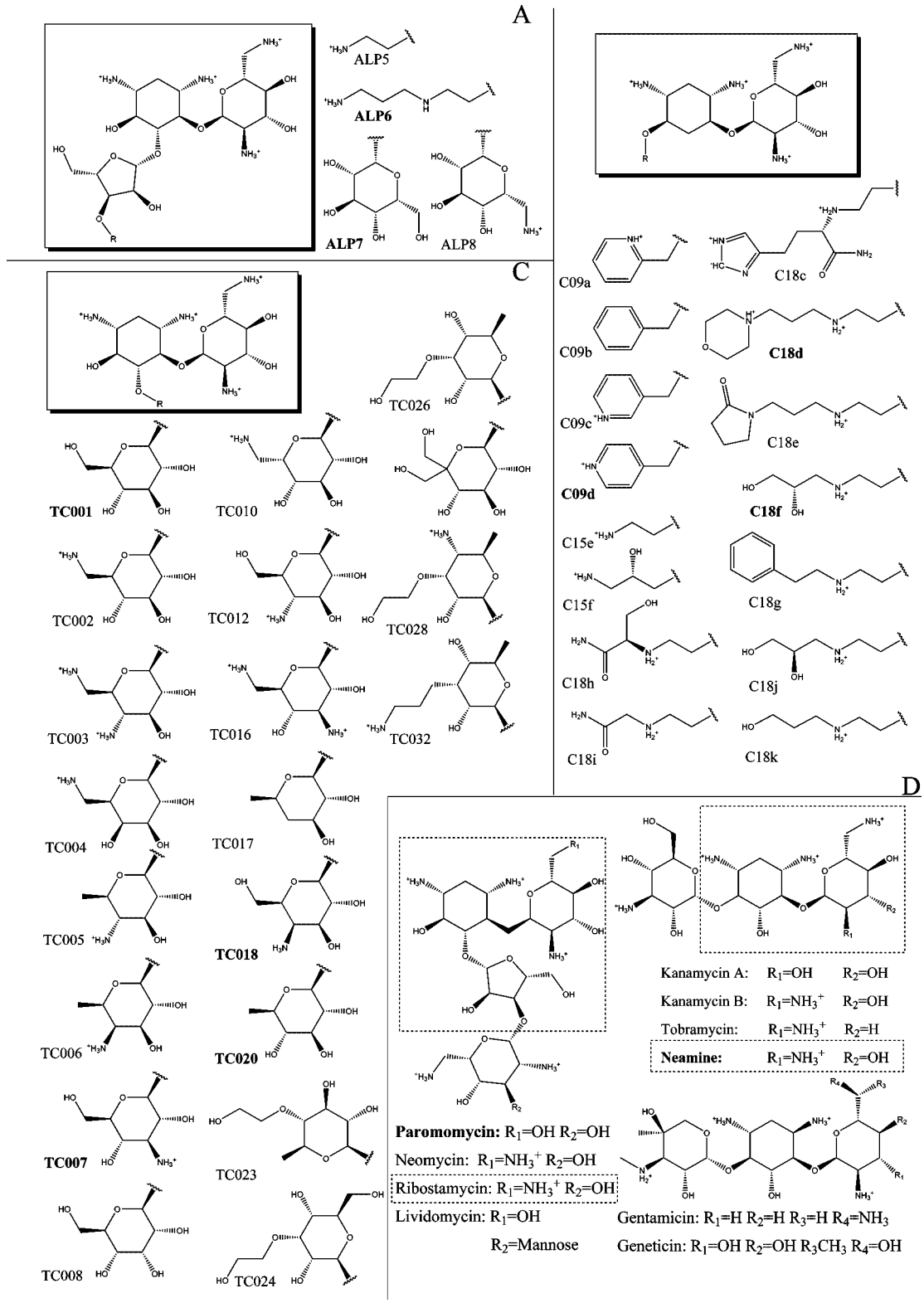

Figure 3. Compounds used for QSAR model development: A — ALP set, B — C set, C — TC set, D —AA set. Compounds whose names are written in bold were used as a test set. Lividomycin and genetecin were only used to validate the QSAR predictivity (see section "Results: QSAR Models").

and a positively charged nitrogen atom (N+), located in the vicinity of O2P oxygen of G1405. Furthermore, in order to provide a proper alignment of an anchoring bond between the fragment and the neamine O5 oxygen, two additional constraints were introduced: one placing a carbon atom at the position of the aminoglycoside C″ carbon, and the second, requiring any atom at the position of the O5 oxygen, that would maintain a single bond with the previous one, while not belonging to the common ring. Also, in order to discriminate fragments extending toward the ring I of neamine, an additional steric feature was placed at its O6′ oxygen.

In the case of 4,6 disubstituted 2-DOS derivatives, the pharmacophore contained the following: a hydrogen bond

Table 1. Features of the Considered Pharmacophores (Figure 2)

feature	status	radius [Å]	color
	4,5 2-DOS Derivatives		
HB acceptor (or hydroxyl)	required	0.50	red
2 HB donors	1 of 2	0.75	green
positive N	required	1.50	blue
C atom	required	0.40	gray
any atom	required	0.40	violet
steric	required	1.50	violet
	4,6 2-DOS Derivatives		
HB donor	required	0.40	green
positive N	required	1.00	blue
C atom	required	0.40	gray
any atom	required	0.40	violet
steric	required	1.75	violet

donor interacting with the O6 oxygen of U1406, a positively charged nitrogen atom located in the vicinity of the O2P oxygen, and an N7 nitrogen of G1405, two linker atoms (defined as above), and a steric feature located at the C5 carbon of U1406. Detailed sizes of the considered features are given in Table 1.

For each pharmacophore, spatial tolerances of its features were established as minimal ones ensuring that during a test search all appropriate fragments of the original aminoglycosides used for pharmacophore development were found in a binding mode corresponding to their position in the parent compound.

Library Preparation. Taking advantage of our screening procedure, based on nonsterically limiting but otherwise rather tight pharmacophoric constraints, apart from a molecular fragment search, we carried out a whole-molecule search, with subsequent fragmentation of promising hits in mind. Such an approach requires inspecting all search results and manual modeling of selected compounds but is relatively easy to perform in reasonable time and allows for expert-based selection of interesting molecular scaffolds.

As a source of fragments we used a subset of fragmentlike structures available from ZINC database repository[37] together with maybridge fragment database (www.maybridge.com), which summed up to 46426 distinct molecular fragments. Structures of whole compounds (90444 in total) were also obtained from ZINC repository. They were selected as representatives of similarity-based clusters (at a 60% Tanimoto cutoff) derived from all available vendors' catalogs, resulting in a set of relatively diverse, druglike molecules. In addition, we also prepared a small set of 13 substituted sugar rings, obtained by cutting glycosidic bonds of eight (see Figure 3) aminoglycoside antibiotics whose crystal structures (bound to A-site) are known. It was used both as a test set to check if our methods can recreate a proper binding mode for known molecules and as a source of elements to construct potentially new aminoglycosides.

All the considered molecular entities were subjected to a common preparation procedure which included the following: addition of hydrogen atoms, determination of the most probable protonation state at pH 7.0, and generation of up to three low energy conformers. It was carried out with the use of the LigPrep and Epik modules of the Schrödinger software suite. The resulting library contained around $25 \cdot 10^4$ records. The subsequent rigid, three-dimensional search was performed, using the UNITY module of Sybyl Software (Tripos).

Hits Assembly and Redocking. Promising molecular fragments, resulting from the pharmacophoric search, were manually extracted (if necessary) from their source molecules and assembled with the neamine moiety. All the molecular modeling was performed with Accelrys DS Visualizer 2.0. The resulting structures were inserted into the binding site (their initial coordinates were based on the known neamine position and substituent alignment into either of the two pharmacophores) and relaxed during a two stage potential energy minimization. In the first stage, apart from the RNA heavy atoms, neamine atoms were kept fixed in their crystallographic positions (taken from PDB: 1J7T; as this file contains models of two A-sites, the one with lower temperature factors was taken, corresponding to PAR46 substructure). In the second stage, the whole ligand was allowed to relax. The potential energy minimization was carried out with the use of Tripos force field and Gasteiger−Hückel charges. The Powell algorithm was used with distance-dependent dielectric constant of 1 and a cutoff for nonbonded interactions of 18 Å. The minimization was terminated when rms displacement between iterations was lower than 0.005 Å. Because it was indicated that specifically located water molecules may play an important role in ligand binding to 16S RNA,[16,19,21] we included some water particles into the binding site (they were not constrained during the minimization). Based on the analysis of crystallographic waters that were common in aligned 16S RNA−ligand complexes and water density distribution obtained in our all-atom, explicit solvent simulations of paromomycin bound to 16S RNA,[38] the following water molecules from 1J7T PDB structure were chosen: 104, 108, 109, 112, 113, 114, 115, 119, 120, 123, 125, 126, 128, 132, 142, 144, 146, 147, 151, 152.

QSAR Model. *Data Sets.* The QSAR model, based on Comparative Molecular Field Analysis (CoMFA)[39] and Comparative Molecular Similarity Indices Analysis (CoMSIA),[40] was derived for ligands whose biological activities were taken from the literature. These ligands were selected in order to cover both O5 and O6 substituted neamine derivatives and to provide biological data that was possible to standardize. The complete data set included the following: 8 aminoglycosides (AA set − Figure 3, D, without lividomycin and Geneticin), 20 pyranmycins containing a variable pyranose ring attached at the O5 of neamine via a β linkage (TC set − Figure 3, C),[29] 15 2,5-dideoxystreptamine O6-ether derivatives (C set − Figure 3, B),[30] and 4 neomycin B derivatives modified in the idose ring (ring IV) − ALP set (Figure 3, A).[26] They displayed a wide range of activities, measured by *in vitro* minimum inhibitory concentrations (MIC − the lowest antibiotic concentration that inhibits the visible bacteria growth after overnight incubation), against standard *E. coli* strain (ATCC 25922). Within each published data set, activities of neomycin B and at least one more standard aminoglycoside were provided as a reference, allowing for standardization of biological data. It should be noted that choosing MIC as an activity descriptor results in predictions regarding biological function of the considered compounds, rather than their direct binding affinity to 16S RNA.

Table 2. Statistical Results for Single Field CoMFA (F) and CoMSIA (C) Models[a]

	CoMFA							CoMSIA				
	FS	FE	FiS	FiE	FpS	FpE	**FHB**	CS	CE	CD	**CA**	**CHD**
q^2	0.41	0.30	0.49	0.23	0.47	0.36	**0.61**	0.52	0.33	0.50	**0.61**	**0.65**
c	3	6	3	3	3	6	**3**	2	2	2	**3**	**3**
SEP	1.3	1.5	1.2	1.5	1.3	1.4	**1.0**	1.2	1.4	1.0	**1.0**	**1.0**
F	64.2	12.3	89.6	75.3	72.3	16.8	**347.8**	48.6	34.4	77.6	**49.5**	**122.7**
r^2	0.86	0.54	0.89	0.88	0.87	0.61	**0.97**	0.82	0.68	0.83	**0.82**	**0.92**
r_p^2	0.74	0.71	0.82	0.61	0.77	0.67	**0.82**	0.56	0.72	0.66	**0.80**	**0.80**

[a] Fields: S — steric, E — electrostatic, D — donor, A — acceptor, HB — H-bond, HD — hydrophobic. q^2 — square of cross-validated (LOO) correlation coefficient at optimal number of components, c — optimal number of components, SEP — standard error of prediction, F — F-test value: $F = r^2/(1 - r^2)$, r^2 — square of non-cross-validated correlation coefficient, r_p^2 — predictive r^2.

Table 3. Progressive Scrambling Results for the Three Best, Single Field Models and Their Combinations[a]

model	c	Q^2	cSDEP	$dq^2/dr_{yy'}^2$	r_p^2
FHB	3	0.55	1.1	0.92	0.82
FHB	4	0.56	1.1	1.00	0.82
CA	3	0.49	1.1	1.12	0.80
CA	4	0.40	1.3	1.36	0.84
CHD	3	0.53	1.1	1.33	0.80
CHD	4	0.47	1.2	1.56	0.74
FHB+CHD	**3**	**0.57**	**1.1**	**0.96**	**0.82**
FHB+CHD	4	0.56	1.1	0.99	0.82
CA+CHD	3	0.49	1.2	1.12	0.80
CA+CHD	4	0.47	1.2	1.53	0.79

[a] c — the considered number of components, $Q^2 - q^2$ value at $s = 0.85$ (degree of correlation between original and perturbed data), cSDEP — standard error of prediction at a given s, $dq^2/dr_{yy'}^2$ —a slope of $q^2(r_{yy'}^2)$ curve at the point s, r_p^2 — predictive r^2.

A consistent data set of 8 aminoglycoside antibiotic activities was taken as a reference.[4] Logarithms of MIC values from all other data sets were shifted by appropriate constant values, determined in each case in order to minimize the sum of squared differences with ln(MIC) for overlapping compounds from the reference data set; this approach provided a unified activity scale for all the considered compounds. Finally, all values were multiplied by −1, and shifted by +10, in order to obtain a scale of positive numbers, whose values positively correlate with activities (Table 4).

The resulting set of 47 compounds was sorted with respect to activity and divided in such a way that every fourth compound was assigned to a test set (11 molecules), while the remaining compounds were assigned to a training set (36 molecules). As a result, both obtained sets contained molecules representing possibly a wide range of activities. The training set was used to construct preliminary QSAR models, while the test set—for their evaluation. The final QSAR model was based on all 47 compounds.

Alignment Procedure. 3D QSAR methods require alignment of considered compounds that represents their relative positions and conformations within the binding site.

Molecules in the AA set (apart from kanamycin B) were aligned directly, by superposition of the available crystal structures of aminoglycosides complexed with the 16S RNA fragment. The alignment was carried out with the use of the atom-based rmsd (Root Mean Square Deviation) fit method (applied to phosphorus atoms of 16S RNA nucleotides that were closer than 5 Å from paromomycin in the PDB 1J7T crystal structure) implemented in SYBYL. Kanamycin B whose structure is not present in the PDB database was modeled using kanamycin A scaffold (PDB 2ESI).

For the molecules of the remaining sets, their sugar ring positions were preliminarily assigned based on maximum common substructure with aminoglycosides from the AA set: neamine moiety in the case of the C set, neamine and ring III of ribostamycin (from PDB 2ET5) in the case of the TC set, and neomycin (from PDB 2ET4) for the ALP set. The core structures were inserted into the binding site, based on alignment of their corresponding PDB structure with PDB 1J7T, in the same way as in the case of molecules of the described above AA set. Then, the core structures were fixed, and conformations of the remaining acyclic side chains were determined as the lowest energy conformers found with the systematic search algorithm. Dihedral angle increments of 5 degrees were used if the number of rotatable bonds was lower than 6, and 10 degrees otherwise. Finally, minimization of entire ligands was performed, using the scheme already described in section "Methods: Hits Assembly and Redocking". Protonation states of all ligands were determined at pH 7.0 (Epik module, Schrödinger), and charges were assigned with the use of the Gastaiger-Hückel method (SYBYL software). Aligned structures of all ligands are presented in Figure 4.

Due to the systematic search procedure, the obtained docking modes should represent the global energy minimum within the applied force field. Thus, such a procedure should provide a consistent data set, suitable for subsequent QSAR model development.

Calculation of Descriptors and Model Development. CoMFA and CoMSIA field descriptors were calculated using standard settings in the SYBYL program. For CoMFA calculations, an sp^3 carbon probe atom with a +1 charge was used. Energy values were truncated to ±30 kcal/mol, and a steric cutoff was applied for evaluation of electrostatic field values. Apart from standard CoMFA fields, indicator, parabolic, and H-bond fields were also evaluated. For CoMSIA calculations, the attenuation factor of the Gaussian function was set to 0.3. In all cases, the grid box dimensions were determined automatically in such a way that the region boundaries were extended at least 4 Å beyond every molecule in all directions, and the grid spacing of 2 Å was used. In total, 12 different fields were calculated (7 CoMFA and 5 CoMSIA fields), corresponding to electrostatic, steric, hydrophobic, and hydrogen bonding properties of the ligands.

QSAR models were developed using regression analysis based on the partial least-squares (PLS) method, with a standard scaling of field values. The initial selection of an optimal number of PLS components (c) was performed on the basis of a leave-one-out (LOO) cross-validation scheme,

Table 4. Experimental MIC Values for Compounds Used for QSAR Model Development[a]

name	MIC [μM]	ACT	pACT	δ
gentamicin	1.6	9.77	9.49	−0.28
ALP6	1.6	9.21	8.66	− 0.55
tobramycin	3.1	9.00	9.42	0.42
neomycin	3.1	8.97	8.48	− 0.49
ALP5	3.1	8.55	8.02	− 0.53
ALP8	3.1	8.55	8.26	− 0.29
kanamycin B	1.85	8.41	9.24	0.83
paromomycin	6.25	7.98	7.83	− 0.15
kanamycin A	12.5	7.59	8.31	0.72
ribostamycin	12.5	7.54	6.96	− 0.58
C18c	4	7.29	6.23	− 1.06
ALP7	12.5	7.16	7.67	0.51
TC005	9	7.11	6.83	− 0.28
TC006	9	7.11	6.64	− 0.47
TC010	9	7.11	7.24	0.13
TC018	12	6.82	6.45	− 0.37
TC028	13	6.74	7.10	0.36
TC002	16	6.54	6.89	0.35
TC003	19	6.36	6.42	0.05
TC020	19	6.36	6.38	0.02
TC012	20	6.31	6.48	0.17
TC029	22	6.22	6.25	0.03
TC004	25	6.09	6.44	0.35
TC007	26	6.05	6.01	− 0.04
TC026	27	6.01	6.07	0.06
TC016	28	5.98	5.85	− 0.13
TC008	29	5.94	5.88	− 0.06
neamine	36	5.85	5.61	− 0.24
TC023	38	5.67	5.80	0.13
TC032	39	5.65	5.66	0.01
TC024	40	5.62	5.79	0.17
TC001	42	5.57	5.95	0.38
TC017	45	5.50	5.88	0.38
C18i	32	5.21	5.12	− 0.09
C18k	32	5.21	5.11	− 0.10
C15e	64	4.52	4.45	− 0.07
C15f	64	4.52	4.56	0.04
C18e	64	4.52	4.41	− 0.11
C18f	64	4.52	4.71	0.19
C18g	64	4.52	4.37	− 0.15
C18h	64	4.52	4.78	0.26
C18j	64	4.52	4.56	0.04
C09a	100	4.07	4.14	0.07
C09b	100	4.07	3.95	− 0.12
C09c	100	4.07	3.94	− 0.13
C09d	100	4.07	4.28	0.21
C18d	100	4.07	4.56	0.49
Geneticin			8.18	
lividomycin			7.68	

[a] ACT — activities expressed as ln(MIC) + Δ_i, where Δ_i was determined for each set in order to standardize experimental data (see section "Methods: QSAR Model"), pACT — predicted activities, δ — residuals.

with the use of the SAMPLS technique implemented in SYBYL. A c value was chosen, for which introduction of an additional component did not increase q^2 (cross-validated correlation coefficient) by more than 10%. Then, the complete model, with a selected number of components, was constructed using a non-cross-validated PLS scheme. Due to a relatively small amount of activity data we decided not to consider models with more than 4 PLS components.

Promising models (with LOO $q^2 > 0.6$ for optimal c number) were further examined, using the progressive scrambling method.[41] Their stability and a final number of components were assessed, based on analysis of Q^2 (q^2 at the critical degree of correlation between original and perturbed data: s), cSDEP (standard error of prediction at a given s), and a slope of $q^2(r^2_{yy'})$ curve (where $r_{yy'}$ denotes a degree of correlation between original and perturbed data) at the point s. For the progressive scrambling tests, 30 scramblings were performed for data records partitioned in a maximum of 10 bins and a minimum of 2 bins, and a standard value of $s = 0.85$ was chosen.

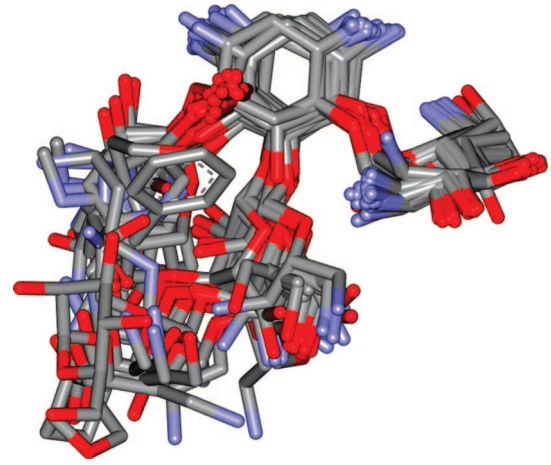

Figure 4. Ligands aligned prior to QSAR model development (both training and test sets). For clarity, hydrogen atoms are not displayed.

An additional, independent model validation was performed by computing activities of 11 molecules from the test set and comparing them with experimental data. The predictive ability of a model was expressed as their correlation coefficient: r^2_p (predictive r^2).

At first, each of twelve, single field models was subjected to statistical analysis and visual inspection of predicted versus experimental activity plots. Then, the fields with a promising performance were combined into more complicated models whose statistical and visual inspection led to selection of a final model. After selecting the best set of descriptors and a corresponding number of components (with the use of the same scheme as described above for single field models), the final model was constructed, based on data from both the training and the test sets. Finally, it was applied to evaluate activities of ligands obtained from the pharmacophoric search.

RESULTS

QSAR Models. Statistical results for the twelve, single field models are given in Table 2. [FHB is in fact a two field model, representing hydrogen bond acceptors and donors. However, in the current software implementation both fields are not separable and thus are referred to as a "single field".] Three models, FHB, CA, and CHD, yielded $q^2 > 0.6$ and $r^2_p > 0.8$, at $c = 3$ each. The first two models are based on hydrogen bonding properties, while the third one—on the distribution of ligands' hydrophobic regions.

The best three single field models and their combinations were subjected to additional analysis with the progressive scrambling technique (Table 3). For each model tests were performed at complexity levels of 2, 3, 4, and 5 components, but the results for both 2 and 5 components were always worse than for 3 or 4, and thus we do not show them in Table 3.

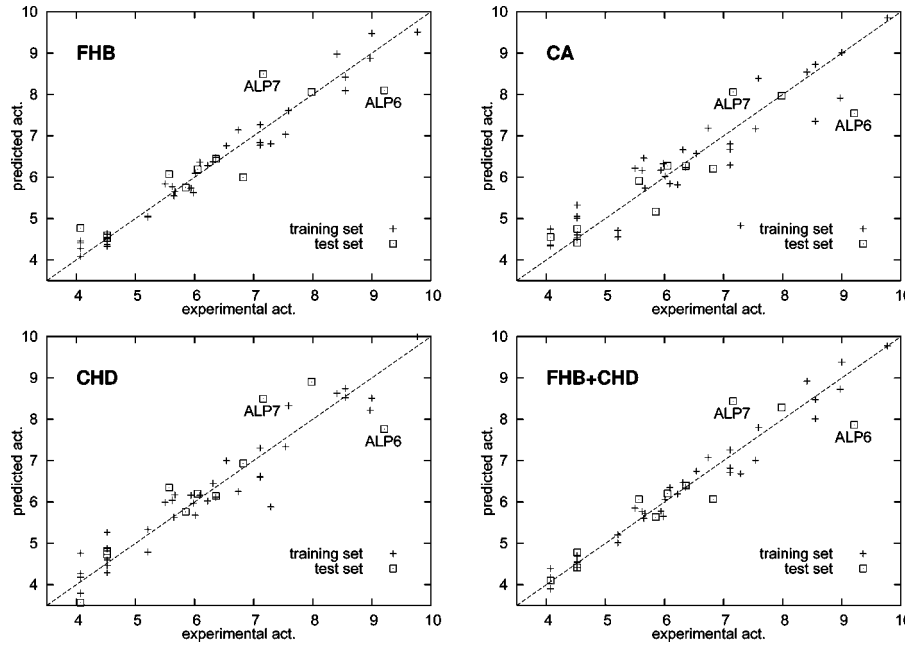

Figure 5. Predicted versus experimental activities for the training set and the test set compounds, for the best three single field models, and the best two field model. FHB — H-bond CoMFA field, CA — acceptor CoMSIA field, CHD — hydrophobic CoMSIA field.

The FHB model turned out to be the best among single field models, with the highest Q^2 values and the $q^2(r^2_{yy'})$ curve slope close to 1.0 at $r^2_{yy'} = 0.85$, suggesting that it is not biased by training data redundancy. Adding a fourth component to the original number of three, that was indicated by the LOO cross-validation test, gives a better performance when the training set is considered alone but does not increase the predictive r^2. The other two models are worse, especially when considering the $dq^2/dr^2_{yy'}$ values, which suggests their higher dependence on accidental correlations in the training data.

As H-bond and hydrophobic fields are not directly correlated, we decided to consider models combining those two kinds of descriptors. In particular, the FHB+CHD model was found to give the best Q^2 for the lowest component number, while still yielding the slope of the $q^2(r^2_{yy'})$ curve close to 1 (Table 3). In comparison to the FHB only model, it also allowed for the inclusion of an additional molecular property for interpretation of the activity data.

Including other single field descriptors, apart from those listed in Table 2, did not improve the FHB+CHD model performance (statistical data not shown), which might have been expected from their standalone results (Table 2). Surprisingly, all models based on electrostatic field (FE, FiE, FpE, and CE) were consistently the worst even though electrostatic interactions were indicated as the most important for aminoglycoside binding to the A-site.[14] However, one should take into account that neamine, carrying four positively charged amino groups and, therefore, responsible for the majority of the electrostatic interaction with RNA, is common for most of the considered compounds (with the exception of paromomycin which is a 6′OH substituted aminoglycoside, carrying a $+3e$ charge on rings I−II. That is why it contributes little to the *variability* of the structure−activity relationship, whose explanation is the main purpose of the QSAR analysis. On the contrary, diverse O5 and O6 substituents are not highly charged but rather contribute to the binding energy by forming specific hydrogen bonds with the surrounding RNA.

Plots of predicted versus experimental activities (Figure 5) for the best three single field models and the FHB+CHD model reveal that in each case two molecules from the test set, ALP6 and ALP7, have their activities, respectively, under- and overestimated. Both ligands are neomycin derivatives and are among the biggest of the considered compounds. They explore relatively worse parametrized regions of the descriptor fields, which may be the reason for the worse predictive performance of the models for these ligands. Neither of the two molecules, however, appears to be a true outlier because including them into the final model results in predicted activities remaining within the accuracy level observed for other compounds (Table 4).

The final model, used to predict activities of the compounds found during the pharmacophore search, was constructed based on the whole available data, combining molecules from both the training and the test sets. Similarly as for the preliminary model, LOO cross-validation and progressive scrambling tests both indicated three components as the best complexity level. It confirms that the training set was indeed representative for the whole considered population of molecules. The obtained statistics were as follows: $q^2 = 0.68$, SEP = 0.91, $F = 259.3$, $r^2 = 0.95$, $Q^2 = 0.62$, cSDEP = 0.98, and $dq^2/dr^2_{yy'} = 0.85$. The contributions of different fields were as follows: FHB: 78% (acceptor field: 38%, donor field: 40%), CHD: 22%.

When one takes into account diversity of the considered compounds, both with respect to their chemical structures and biological activities, the model reproduces the experimental data quite well. As shown in Table 4, in most cases the differences between the actual and predicted activities are well below 1.0, while the whole range of activity scale is close to 6 units. We expect that the model when applied to molecules resulting from the pharmacophoric search should be able to properly discriminate between active and inactive ligands. This ability can be exemplified by the case

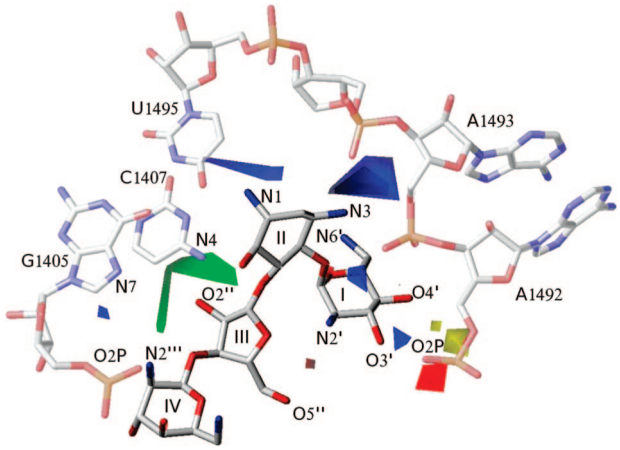

Figure 6. H-bond field contour map. Green and yellow: regions where hydrogen bond donors on the receptor would be favored or disfavored, respectively, for ligand activity. Blue and red: regions where hydrogen bond acceptors on the receptor would be favored or disfavored, respectively, for ligand activity.

of two aminoglycosides: Geneticin and lividomycin whose crystallographic structures in the complex with the A-site are known (PDB: 1MWL and 2ESJ, respectively), but reliable MIC values against the standard *E. coli* ATCC 25922 strain were not found in literature. The predicted activities of 8.18 for Geneticin and 7.68 for lividomycin place them in the active group, where they should indeed belong.

3D QSAR Contour Maps. Contour maps of the H-bond CoMFA field contribution are presented in Figure 6. The green contour of the acceptor field corresponds to a region from where a hydrogen bond should be directed toward the ligand's acceptor group, in order to increase its activity. The contour is focused on the N4 nitrogen of C1407. This nitrogen is involved in direct hydrogen bonds with all active 4,5 2-DOS substituted aminoglycoside antibiotics.[19] It also maintains close contacts (with less than 3 Å distance) with oxygen atoms belonging to ring III of 4.6 2-DOS substituted aminoglycosides. As natural aminoglycosides are the most active group among the compounds considered in the QSAR model development, the positive correlation between the presence of this hydrogen bond and activity is, indeed, expected. It is also interesting to note that the N4 nitrogen of C1407 is one of the very few hydrogen bond donors involved in direct contacts with aminoglycosides since the compounds of this family are mostly hydrogen bond donors themselves.

Yellow and red contours in Figure 6, located in the vicinity of the O2P oxygen of A1492, correspond to regions where, respectively, the hydrogen bond donors and acceptors in the receptor are disfavored for ligand activity. Their presence in this location seems to originate from the fact that the two most active ligands, gentamicin and tobramycin, lack a hydroxyl group at the 3′ position of neamine ring I. Such a group is present in all other, less active compounds and is involved in a hydrogen bond with an O2P oxygen of A1492. Even though a set of substituents present in the neamine moiety, which includes the 3′ hydroxyl group (see Figure 1), seems to be optimal for its binding to the A-site,[27] statistics based on the particular data set used here indicate the 3′ hydroxyl as disfavored for ligand activity. However, since all newly constructed molecules have the 3′ hydroxyl group, the influence of the two considered H-bond field regions on the final QSAR model outcome should not affect their predicted relative activities.

Blue contours correspond to regions where hydrogen bond acceptors are favored for ligand activity. The biggest contour is located near the N3 nitrogen of neamine ring II. This nitrogen atom is responsible for the most conservative contacts between aminoglycosides and RNA, contributing to hydrogen bonds with the N7 nitrogen and the O2P oxygen of G1494 (not shown in Figure 6) and the O1P oxygen of A1493. Also, carrying a positive charge, the N3-amino group seems to fit into a particularly strong electrostatic field caused by negatively charged RNA. This fact correlates with a significant concentration of positive ions in this area observed in molecular dynamics simulations of the bare A-site.[38]

While a dominant role of the N3 nitrogen itself in aminoglycoside binding to RNA is undoubtful,[4,16,21] the importance of its neighboring region in QSAR analysis may be somewhat surprising. This N3 nitrogen is found in all the considered molecules as the part of neamine, and hence, its presence should not explain differences in their activities. The observed result may reflect the sensitivity of the QSAR model to small differences in relative orientations of ligands: those with high binding affinity (especially natural aminoglycosides) were more stable during energy minimization phase of the ligand set preparation, while the others might have undergone slightly greater changes, leading to translocation of their N3 nitrogen from the initial location. Indeed, N3 nitrogen atoms of all molecules docked into the A-site for subsequent QSAR model development are scattered in a sphere of 1 Å radius, while all N3 nitrogen atoms of the ten most active compounds occupy a subsphere of only 0.4 Å radius. It should be also noted that a proper, precise positioning of rings I and II is crucial for aminoglycoside activity—their displacement caused either by mutations of the surrounding nucleotides[42,43] or by neamine chemical modifications[5] is considered as one of the major mechanisms involved in bacterial resistance. Following this reasoning, the considered blue contour should be regarded as a result of the QSAR model sensitivity to optimal arrangement of the hydrogen bonding pattern which is achieved by molecules that can fit properly into the binding site without major conformational strain. Similar conclusions should also apply to smaller donor field blue contours observed near N1 and N2′ nitrogen atoms of neamine.

A small blue region is also visible between the O2P oxygen and the N7 nitrogen of G1405. It corresponds to the hydrogen bond that is formed with one (or both) of these atoms by aminoglycoside nitrogen atom, attached either to ring IV (in 4,5 2-DOS family) or to ring III (in 2,6 2-DOS family). As this bond (or two bonds) is seen in most of the experimental structures of complexes of aminoglycosides with the A-site (a nitrogen donor atom in this area was also deemed important in both constructed pharmacophores), it is expected to correlate positively with ligands' activity.

Contours of the hydrophobic CoMSIA field are presented in Figure 7. Blue regions, where the presence of hydrophilic groups is expected to positively correlate with ligand activity, indicate the importance of contacts with polar atoms of G1405 (O2P oxygen and N7 nitrogen) as well as C1407 (N4 nitrogen). Interestingly, one of the gray contours, corresponding to the area where nonpolar groups are favored, is located in a solvent exposed region, right in the middle

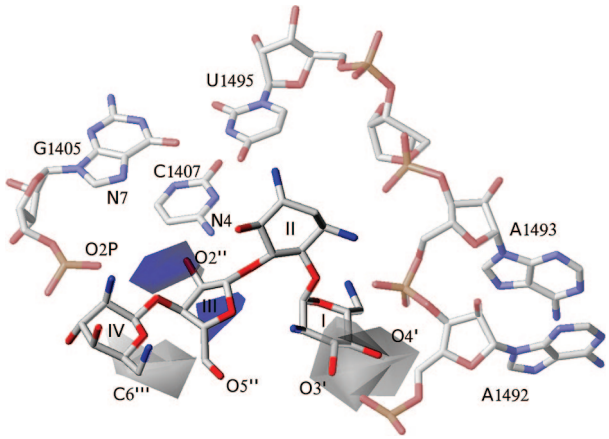

Figure 7. Hydrophobic field contour map. Contours correspond to regions where hydrophobic (gray) or hydrophilic (blue) groups in the ligand are favorable for its activity.

between polar phosphates of G1405 and A1492. Possibly, nonpolar fragments of bound molecules can exist in this region maintaining minimal contact with charged phosphate groups, while still providing a necessary scaffold for polar substituents. It should be noted that the RNA binding site lacks any hydrophobic pockets where nonpolar groups could preferably gather, and hence the whole variability of the hydrophobic field is shifted toward values representative for more hydrophilic regions.

A second region of the hydrophobic field that corresponds to its positive correlation with ligand activity is located near O3′ and O4′ oxygens of neamine ring I. Similarly as in the case of H-bond field regions present in this area (yellow and red contours in Figure 6), these regions are due to the fact that the two most active compounds: gentamicin and tobramycin, in contrast to all the other ligands, lack two (or one, respectively) hydroxyl groups in these positions. Again, this element of the QSAR model should have no influence on relative activities of the screened compounds.

Search Results. The two pharmacophoric searches resulted in initial numbers of 39 and 440 hits for O5 and O6 pharmacophores, respectively. Upon manual selection, 7 O5 and 14 O6 substituents were subjected to further analysis (Figure 8). After their assembly with neamine scaffold, they were inserted into the binding site, and their conformation was further optimized, as described in the section "Methods: Hits Assembly and Redocking". The number of hits achieved in each search and the corresponding acceptance ratios reflect differences in complexity of both pharmacophores: the O5 pharmacophore is more tight than the O6, but once a molecule satisfies its criteria, it is more likely to represent a promising scaffold.

The resulting set contains quite diverse molecules. Most of the selected neamine substituents carry a single, charged amino group which gives a total charge of $+5e$ per compound. Such a result is expected because the positive nitrogen feature was present in both O5 and O6 pharmacophores. It should be noted, that while such a large total charge is disadvantageous for the ADMET (Absorption, Distribution, Metabolism, Elimination, and Toxicity) profile of molecules, it is observed among all natural A-site ligands and is indicated as important for their specific and high affinity binding.[19]

Five molecules resulting from the pharmacophoric search (**1**−**4** and **15**) represent linear or branched amino alcohols. Similar neamine or dideoxystreptamine derivatives were already considered in experimental studies,[27,30,32] yielding low to moderate activities toward bacterial ribosomes. Accordingly, activities predicted here for this class of ligands remain in the middle of the obtained activity scale.

In most of the hits, among them the most active ones, the neamine core is accompanied by a single ring substituent. It seems that this type of structure provides an optimal framework for the necessary hydrogen bond pattern. The larger, bulky substituents tend to achieve lower predicted activities similar as in naturally occurring aminoglycosides. Members of the 4,6 2-DOS linked family consist of only three rings, of which a six membered ring III, attached to the neamine core, provides a scaffold for interacting hydroxy and amino groups. In the case of the 4,5 family, although rings IV or V are often present, specific hydrogen bonds with RNA are rather limited to ring III. The other rings, although important for activity (in particular ring IV), provide less specific and more labile contacts.[44,45]

Four top ranked compounds have potential activities greater than 7.0, which places them among the best 25% of ligands used for model development. Activities comparable to the most active aminoglycosides should not be expected since the search was aimed at diverse, new scaffolds, representing candidates for potential lead compounds, rather than tuned for optimization of already active inhibitors.

Among four, potentially best compounds there are two O5 and two O6 neamine derivatives (Figure 9). Interestingly, both O6 derivatives (compounds **10** and **5**) can form hydrogen bonds with the N4 nitrogen of C1407. The QSAR model indicated this hydrogen bond as important for activity, but it was not specified in the O6 pharmacophore (Figure 2, b). Furthermore, in both O6 derivatives and in one O5 derivative (compound **16**) the carbonyl oxygen is an acceptor of this bond, which should provide stronger interaction than when a hydroxyl oxygen acts as acceptor which is observed in natural aminoglycosides.

Substituents in all four compounds have a nitrogen atom that should be positively charged at pH 7.0 (as indicated by the performed pK_a calculations). This nitrogen maintains interactions with the O2P oxygen and/or the N7 nitrogen of G1405 which, according to the QSAR model, positively contributes to ligand activity. Also, as expected from pharmacophore construction, both O6 derivatives have hydroxyl groups interacting with the O6 oxygen of G1405, while both O5 derivatives interact via their hydroxyl groups with the N7 nitrogen of G1491.

Due to the presence of the sulfonic group, the compound **5** can maintain an intramolecular hydrogen bond between the O6 substituent and the O5 oxygen of neamine ring II. Such intramolecular hydrogen bonds are also seen in natural aminoglycosides. They are believed to contribute to resistance to enzymatic inactivation of the drugs, by favoring conformation appropriate for RNA binding but not suitable for binding pockets of enzymes involved in bacterial resistance.[46]

SUMMARY

We presented a procedure allowing for selection and subsequent evaluation of novel, potentially promising com-

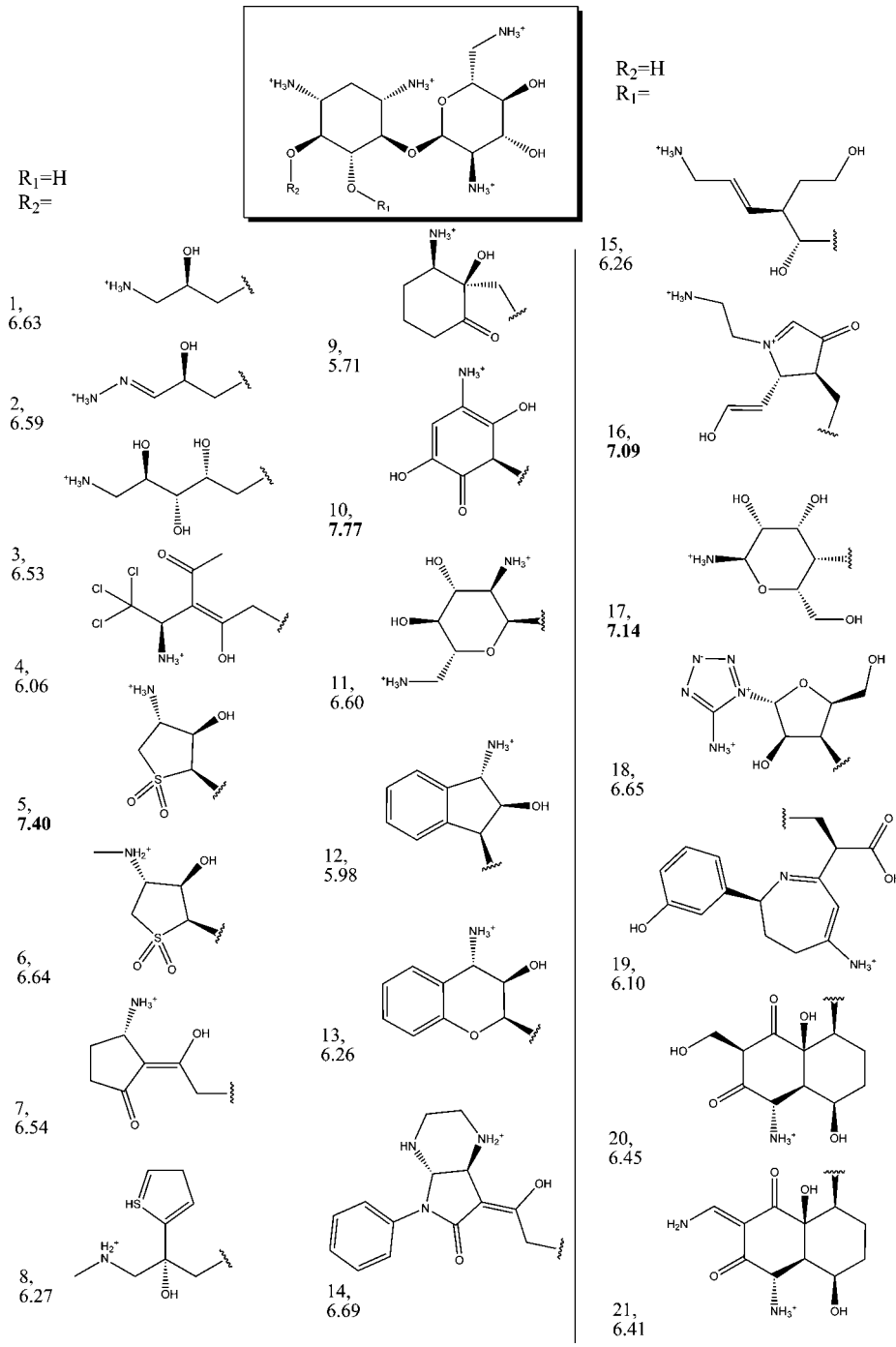

Figure 8. O6 (left) and O5 (right) neamine substituents selected from the pharmacophoric search. Following the ID numbers, activities of assembled ligands indicated by QSAR model are provided.

pounds targeting the 16S RNA A-site. The procedure was based on a pharmacophoric search of a fragment library, followed by the assembly of successful hits with the neamine scaffold and estimation of biological activity of the proposed compounds with a developed 3D-QSAR model.

As current methods for small molecule docking and scoring in nucleic acids are still in the early phases of development, our approach demonstrates an alternative way for computer aided design and ranking of RNA ligands. It should be emphasized that the considered 16S RNA A-site fragment is particularly suitable for such an approach: 1) there are a lot of structural data, giving insight into important aspects of specific RNA−ligand interactions, which enables constructing pharmacophores for both 4,5 and 4,6 substituted 2-DOS derivatives, 2) the neamine scaffold is conserved among aminoglycosides and in each case adopts a virtually identical position within the binding site, which allows predicting the binding modes for the proposed ligands, and 3) the ability to properly align the considered molecules together with relatively vast biological data enable constructing a reliable 3D-QSAR model, which can be used for ranking the new hits.

The analysis of the available types of CoMFA and CoMSIA field descriptors shows that when molecules with distinct substituents to the common neamine core are considered, differences in their activities depend mostly on specific hydrogen bond patterns and the distribution of hydrophobic and hydrophilic fragments, rather than electrostatic interactions. While electrostatic interactions were indicated as the most important

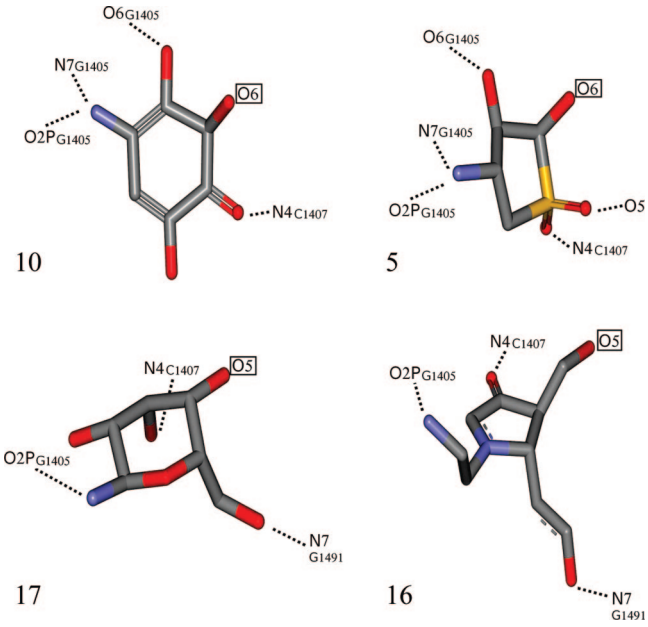

Figure 9. Interactions of O5 and O6 substituents of the four most active compounds indicated by the QSAR model with the surrounding RNA.

for aminoglycoside binding to RNA, such a result can be justified by the fact that the major contribution to those interactions comes from the +4*e* charge carried by the neamine moiety, which is identical in most of the considered compounds, and therefore does not contribute much to variability in their activities. In contrast, hydrogen bonding properties of the neamine substituents are diverse and thus responsible for differences in ligand−RNA interactions.

In general, the obtained QSAR model reproduces well the available biological data for a set of quite distinct compounds, ranging from potent aminoglycosides to inactive representatives of the C set. It seems that the model should be able to discriminate between potentially active and inactive candidates resulting from the pharmacophoric search. The predicted activities of the best four compounds (two 4,5 and two 4,6 disubstituted 2-deoxystreptamine derivatives) remain within the range of activity of the less potent aminoglycoside antibiotics. Because our search was aimed at diverse, new scaffolds, not particularly optimized for interactions with RNA, their further improvement is still possible.

ACKNOWLEDGMENT

The authors acknowledge support from the University of Warsaw (115/30/E-343/BST1345/ICM/2008 and ICM-G31-4), the Polish Ministry of Science and Higher Education (3T11F00530, 2006−2008), the Fogarty International Center (National Institutes of Health Research Grant no R03 TW07318), and the Foundation for Polish Science (Focus program).

REFERENCES AND NOTES

(1) Walsh, C. *Nature* **2000**, *406*, 775–781.
(2) Knowles, D. J. C.; Foloppe, N.; Matassova, N. B.; Murchie, A. I. H. *Curr. Opin. Pharmacol.* **2002**, *2*, 501–506.
(3) Hermann, T. *Curr. Opin. Struct. Biol.* **2005**, *15*, 355–366.
(4) *Aminoglycoside antibiotics. From chemical biology to drug discovery*; Arya, D. P., Ed.; John Wiley & Sons Inc.: Hoboken, NJ, 2007.
(5) Magnet, S.; Blanchard, J. S. *Chem. Rev.* **2005**, *105*, 477–498.
(6) Fourmy, D.; Recht, M. I.; Blanchard, S. C.; Puglisi, J. D. *Science* **1996**, *274*, 1367–1371.
(7) Carter, A. P.; Clemons, W. M.; Brodersen, D. E.; Morgan-Warren, R. J.; Wimberly, B. T.; Ramakrishnan, V. *Nature* **2000**, *407*, 340–348.
(8) Vicens, Q.; Westhof, E. *Structure* **2001**, *9*, 647–658.
(9) Vicens, Q.; Westhof, E. *Chem. Biol.* **2002**, *9*, 747–755.
(10) Vicens, Q.; Westhof, E. *J. Mol. Biol.* **2003**, *326*, 1175–1188.
(11) Lynch, S. R.; Gonzalez, R. L.; Puglisi, J. D. *Structure* **2003**, *11*, 43–53.
(12) Hendrix, M.; Priestley, E. S.; Joyce, G. F.; Wong, C. H. *J. Am. Chem. Soc.* **1997**, *119*, 3641–3648.
(13) Hermann, T.; Westhof, E. *J. Mol. Biol.* **1998**, *276*, 903–912.
(14) Pilch, D. S.; Kaul, M.; Barbieri, C. M.; Kerrigan, J. E. *Biopolymers* **2003**, *70*, 58–79.
(15) Barbieri, C. M.; Srinivasan, A. R.; Pilch, D. S. *J. Am. Chem. Soc.* **2004**, *126*, 14380–14388.
(16) Pilch, D. S. *Top. Curr. Chem.* **2005**, *253*, 179–204.
(17) Yang, G.; Trylska, J.; Tor, Y.; McCammon, J. A. *J. Med. Chem.* **2006**, *49*, 5478–5490.
(18) Moazed, D.; Noller, H. F. *Nature* **1987**, *327*, 389–394.
(19) François, B.; Russell, R. J. M.; Murray, J. B.; Aboul-ela, F.; Masquida, B.; Vicens, Q.; Westhof, E. *Nucleic Acids Res.* **2005**, *33*, 5677–5690.
(20) Zhou, J.; Wang, G.; Zhang, L.-H.; Ye, X.-S. *Med. Res. Rev.* **2007**, *27*, 279–316.
(21) Vicens, Q.; Westhof, E. *Biopolymers* **2003**, *70*, 42–57.
(22) Wong, C.-H.; Hendrix, M.; Manning, D.; Rosenbohm, C.; Greenberg, W. *J. Am. Chem. Soc.* **1998**, *120*, 8319–8327.
(23) Vourloumis, D.; Takahashi, M.; Winters, G. C.; Simonsen, K. B.; Ayida, B. K.; Barluenga, S.; Qamar, S.; Shandrick, S.; Zhao, Q.; Hermann, T. *Bioorg. Med. Chem. Lett.* **2002**, *12*, 3367–3372.
(24) Barluenga, S.; Simonsen, K. B.; Littlefield, E. S.; Ayida, B. K.; Vourloumis, D.; Winters, G. C.; Takahashi, M.; Shandrick, S.; Zhao, Q.; Han, Q.; Hermann, T. *Bioorg. Med. Chem. Lett.* **2004**, *14*, 713–718.
(25) Zhou, Y.; Gregor, V. E.; Sun, Z.; Ayida, B. K.; Winters, G. C.; Murphy, D.; Simonsen, K. B.; Vourloumis, D.; Fish, S.; Froelich, J. M.; Wall, D.; Hermann, T. *Antimicrob. Agents Chemother.* **2005**, *49*, 4942–4949.
(26) Alper, P.; Hendrix, M.; Sears, P.; Wong, C.-H. *J. Am. Chem. Soc.* **1998**, *120*, 1965–1978.
(27) Greenberg, W.; Priestley, E.; Sears, P.; Alper, P.; Rosenbohm, C.; Hendrix, M.; Hung, S.-C.; Wong, C.-H. *J. Am. Chem. Soc.* **1999**, *121*, 6527–6541.
(28) Elchert, B.; Li, J.; Wang, J.; Hui, Y.; Rai, R.; Ptak, R.; Ward, P.; Takemoto, J. Y.; Bensaci, M.; Chang, C.-W. T. *J. Org. Chem.* **2004**, *69*, 1513–1523.
(29) Li, J.; Wang, J.; Czyryca, P. G.; Chang, H.; Orsak, T. W.; Evanson, R.; Chang, C.-W. T. *Org. Lett.* **2004**, *6*, 1381–1384.
(30) Vourloumis, D.; Winters, G. C.; Simonsen, K. B.; Takahashi, M.; Ayida, B. K.; Shandrick, S.; Zhao, Q.; Han, Q.; Hermann, T. *ChemBioChem* **2005**, *6*, 58–65.
(31) Wang, J.; Li, J.; Chen, H.-N.; Chang, H.; Tanifum, C. T.; Liu, H.-H.; Czyryca, P. G.; Chang, C.-W. T. *J. Med. Chem.* **2005**, *48*, 6271–6285.
(32) Haddad, J.; Kotra, L. P.; Llano-Sotelo, B.; Kim, C.; Azucena, E. F.; Liu, M.; Vakulenko, S. B.; Chow, C. S.; Mobashery, S. *J. Am. Chem. Soc.* **2002**, *124*, 3229–3237.
(33) Foloppe, N.; Chen, I.-J.; Davis, B.; Hold, A.; Morley, D.; Howes, R. *Bioorg. Med. Chem.* **2004**, *12*, 935–947.
(34) Moitessier, N.; Westhof, E.; Hanessian, S. *J. Med. Chem.* **2006**, *49*, 1023–1033.
(35) Morley, S. D.; Afshar, M. *J. Comput.-Aided Mol. Des.* **2004**, *18*, 189–208.
(36) Kang, X.; Shafer, R. H.; Kuntz, I. D. *Biopolymers* **2004**, *73*, 192–204.
(37) Irwin, J. J.; Shoichet, B. K. *J. Chem. Inf. Model.* **2005**, *45*, 177–182.
(38) Romanowska, J.; Setny, P.; Trylska, J. *J. Phys. Chem. B* **2008**, *112*, 15227–15243.
(39) Cramer, R. D.; Patterson, D. E.; Bunce, J. D. *J. Am. Chem. Soc.* **1988**, *110*, 5959–5967.
(40) Klebe, G.; Abraham, U.; Mietzner, T. *J. Med. Chem.* **1994**, *37*, 4130–4146.
(41) Clark, R. D.; Fox, P. C. *J. Comput.-Aided Mol. Des.* **2004**, *18*, 563–576.
(42) Pfister, P.; Hobbie, S.; Vicens, Q.; Böttger, E. C.; Westhof, E. *ChemBioChem* **2003**, *4*, 1078–1088.
(43) Hobbie, S. N.; Pfister, P.; Brüll, C.; Westhof, E.; Böttger, E. C. *Antimicrob. Agents Chemother.* **2005**, *49*, 5112–5118.
(44) Hobbie, S. N.; Pfister, P.; Brüll, C.; Sander, P.; Franois, B.; Westhof, E.; Böttger, E. C. *Antimicrob. Agents Chemother.* **2006**, *50*, 1489–1496.
(45) Vaiana, A. C.; Westhof, E.; Auffinger, P. *Biochimie* **2006**, *88*, 1061–1073.
(46) Bastida, A.; Hidalgo, A.; Chiara, J. L.; Torrado, M.; Corzana, F.; Prez-Caadillas, J. M.; Groves, P.; Garcia-Junceda, E.; Gonzalez, C.; Jimenez-Barbero, J.; Asensio, J. L. *J. Am. Chem. Soc.* **2006**, *128*, 100–116.

CI800361A